

9. DEVELOPMENT OF THE ELEVATION DRIVE ASSEMBLY

FOR ORBITING SOLAR OBSERVATORY I (EYE)

By W. F. Sharpe and M. C. Olson

Hughes Aircraft Co., Space & Communications Group

And B. W. Ward, NASA, Goddard Space Flight Center

SUMMARY

The requirements for pointing accuracy, friction, and power for the elevation drive assembly (EDA) of an orbiting space observatory are discussed briefly. A description of the components making up the assembly is presented. Special features requiring development testing prior to unit fabrication are more fully described together with a review of the test programs conducted and results obtained.

INTRODUCTION

The overall objective of the Orbiting Solar Observatory program is to conduct experiments in solar physics and celestial astronomy above the earth's atmosphere. Purpose of the experiments, in general, is to measure the intensity and variations of radiations from the sun and celestial bodies in the ultraviolet, X-ray, and gamma ray wavelengths. The specific mission of OSO-I, shown in Figure 1, is to investigate the sun's lower corona, the chromosphere, and their interface in the X-ray and ultraviolet spectral regions to better understand the transport of energy from the photosphere into the corona. The elevation drive assembly rotates the sun pointed spectrometers referred to herein as the Pointed Instruments Assembly (PIA).

REQUIREMENTS

Inherent precision pointing capability is provided by closed-loop control utilizing the PIA sun sensor. The primary difficulties experienced in designing a suitable elevation drive mechanism which will achieve the required fine pointing capability are misalignments, bearing, and torque variations. The torque variations occur in the bearings and the flexible cables which cross the gimbal axis. Stiction (breakaway friction) of the bearings is especially

important. Maintaining the inertial position of the PIA in the event of vehicle nutation or platform wobble is facilitated by the inherent stability of the high inertia PIA and the use of a low-friction gearless direct drive. The servo has only to compensate for bearing friction to hold the PIA inertially stationary.

The basic requirements are summarized in Table 1. Meeting the pointing stability requirement and the attendant motion and accuracy requirements depends on the performance of the bearing system. Computer simulation of the vehicle and PIA dynamics has established the maximum acceptable friction torque as eight in-oz to meet the one arcsec jitter requirement. The ability of the ADA mechanism to meet these stringent requirements following the launch environment is the key element in achieving a successful mission.

Power requirements are important for two reasons. These are 1) to minimize the demands on the spacecraft power bus, and 2) to keep the power dissipation in the drive assembly at favorable levels to maintain good thermal balance within the unit and minimize thermal distortion in the structure that would affect the alignment references or the bearing friction.

An important consideration in regard to drive torque requirements is the flexing of wires or cables that must cross the gimbal axis. Since only five degrees travel is required, the use of slip rings is not necessary. The design selected for power and signal transfer to the experiment package uses two flat contour cables, installed in a manner to provide a rolling action as the gimbal rotates.

DESCRIPTION

The elevation drive assembly, shown in Figure 2, consists of the following elements:

- A. Yoke - This is an aluminum structure which provides mounting for the spacecraft solar panel and the azimuth reference assembly. The outer bearing races, the motor housing, the position transducer housing, and one end of the flexible cable assemblies are attached to this structure.
- B. Gimbal Saddle - This U-shaped aluminum part essentially forms the shaft of the rotating gimbal. The experiment saddle, bearing inner races, PIA sun sensor, remote multiplexers, remote command decoders, position transducer and motor rotors, and the other end of the flexible cables attach to this part.

- C. Experiment Saddle - This titanium box-shaped structure mounts on the gimbal saddle. The two pointed instruments are attached to the saddle as are the mechanisms for performing and maintaining the coalignment of the pointed instruments.
- D. Bearings - Two oil-lubricated angular contact ball bearings, preloaded by dual flexure springs, provide low and consistent torque over the limited range of rotation.
- E. Motor - A limited-rotation brushless DC motor produces the torque required to position the pointed instruments assembly.
- F. Position Transducer - A variable reluctance differential transformer signal generator furnishes an output signal proportional to the angular position of the PIA. The input voltage is transformed to either an in-phase or out-of-phase relationship to the primary voltage at an amplitude proportional to the rotation from the null position.
- G. Launch Lock Assembly - This is a mechanism with pyrotechnic separation nuts used to hold the PIA during launch and to release it for in-orbit operation. Two separation nuts are provided; the firing of either or both nuts will release the launch lock.
- H. Flexible Cable Assemblies - These flat cables provide the electrical path for power and signal conductors across the gimbal axis.
- I. Coalignment Adjustment Mechanism - These devices, installed within the experiment saddle, furnish azimuth and elevation adjustments necessary to coalign the pointed instruments. The adjustments are made when the instruments are installed; once adjusted, the instruments are locked in place for subsequent operation.

SPECIAL FEATURES

The elevation drive assembly includes several special features which are of such importance to spacecraft operation that special tests were required prior to assembly of the first unit.

A. Launch Lock Mechanism

During the launch environment the experiments, experiment saddle, and gimbal saddle are caged by two pivoted launch lock assemblies that tie the gimbal saddle to the bottom yoke structure (Figure 3). Squib-

actuated explosive nut assemblies are used to attach the clamp locks to the gimbal saddle base. The tie rod mechanism is designed so that should either one of the two explosive nuts fail to fire both clamps will still be released from the gimbal saddle. The operation is illustrated in Figure 4, which shows the locked position and the unlocked position with one nut or both nuts actuated. After the nuts are actuated, the clamp assemblies are rotated out of the way by means of kickoff springs in the clamp and torsion springs located at the pivot joints. Crushable honeycomb material is used as a clamp stop to cushion the impact as the clamp strikes the clamp stops.

A model of the launch lock mechanism was constructed and tested in order to evaluate the release action. The test sequence consisted of firing one nut, then the other, and then both nuts together. After each firing, the crushable honeycomb material was replaced. Each test sequence was conducted five times for a total of 15 release actuations (20 nut firings, total). High speed motion pictures were taken of each firing.

Results were satisfactory except that in one instance the clamp did not clear the threaded end of the tie rod upon release, causing one clamp to remain partially engaged to the saddle. It was also noted during the tests that the honeycomb shock absorber material did not crush as much as expected so that the clamp did not move far enough to permit full six degrees rotation of the gimbal saddle. These problems were corrected by adding a counterbore in the clamp and by reducing the thickness of the honeycomb material by 0.28 inch.

B. Alinement Mechanism

The alinement mechanism is provided so that both the upper experiment and the lower experiment can be pointed at the same sun position. The mechanism is shown in Figure 5. The experiments must be coaligned within five arcseconds and cannot shift more than an additional five arcseconds as a result of the launch environment and temperature excursions. The Paris experiment is hard mounted to the experiment saddle with no adjustment. The Colorado experiment is adjusted in azimuth and elevation as follows:

1. A tapered, rotatable shim is mounted between the experiment and the experiment saddle. The shim can be rotated 30 degrees to provide an elevation adjustment of two minutes with a taper of $0^{\circ} 4'$. Required shim rotation for a five arcsecond adjustment is therefore 1.2 degrees.

2. Azimuth adjustment is achieved by means of a differential screw which links the experiment saddle to the experiment. The differential threads are 27 per inch and 28 per inch. One revolution of the differential screw results in a motion of

$$\frac{1}{27} - \frac{1}{28} = .0013 \text{ inch per turn}$$

At an arm length of 14 inches, the rotation produced is

$$\frac{.0013 \text{ in.}}{\text{Turn}} \times \frac{1}{14 \text{ in.}} \times \frac{57.3 \text{ deg.}}{\text{Rad}} \times \frac{3600 \text{ sec}}{\text{deg.}} = 19 \text{ arcsec per turn}$$

Alignment tests were conducted to determine the repeatability of the mechanism, the resolution of the adjustment, thermal effects over the expected temperature range of 40° to 100° F, and the effect of the launch induced thrust axis load on the coalignment mechanism.

C. Torque and Torque Variation

The major requirements for the ball bearings are low and consistent friction at slow speeds to minimize control loop errors. A small diameter bearing has minimum friction torque because the rolling friction forces act at a small radius. The desire for consistent friction favors use of a small ball diameter on a large diameter race so that small shaft displacements commanded can cause the ball to roll. Should the ball size be too small, contaminant particles will cause inconsistent torque when encountered. A compromise is therefore required. The 11/16-inch ball diameter is large compared with expected contaminants, but the ball is reasonably small compared with the 2.9-inch pitch diameter. The bearing installation is shown in Figure 6.

The friction level for rolling the pair of bearings is less than three in-oz. The friction torque is almost independent of viscous effects because the velocity is low and the temperature range is limited. The ratio of static-to-rolling friction is of major importance to the control system performance. This ratio is made up of two contributing factors. The constant or reproducible factor inherent to ball bearings is the smaller contributor, while the random torque component due to ball and retainer interaction is more significant. This random component is difficult to evaluate analytically and was therefore defined through engineering tests.

Breakaway friction tests were conducted using bearings similar to those planned for the flight vehicle. Direct incremental loading of

a beam attached to the bearing shaft was the method used to obtain breakaway torques. Gravity effects positioned the retainer against the balls and the inner race outside diameter to such an extent that test irregularities became a problem. By changing the bearing shaft from horizontal to vertical, the irregularities were eliminated.

Additional tests conducted with the bearing shaft vertical resulted in breakaway torque of less than 50% of the values recorded in the horizontal position. Breakaway torque was 1.6 in-oz with 16 pounds preload and 2.05 in-oz with 30 pounds preload.

To obtain running friction, the fixture was positioned with the bearing shaft vertical with a preload of 16 pounds. Tests were run at rotational speeds of 0.010 and 0.046 degree per second, obtained by using a Genisco rate table and a 20:1 ratio pulley system. Average running torque was 0.80 in-oz through an arc of 30°. Plots of measured torque are shown in Figure 7. The results indicated the following:

1. The torque characteristics of the balls and race are repeatable and can be used as a reference.
2. At the low levels the torque is independent of rate of rotation and viscous effects are not important.

An attempt was made to measure the flexible cable torque, but this torque was so small that it could not be identified within the variations of bearing fixture torque. An estimate of cable torque would be less than 0.5 in-oz.

PROBLEM AREAS

Several problem areas came to light and were resolved during the development program:

1. Shaft stops, as shown in Figure 8, were added to both the microsyn and motor sides of the yoke to prevent the delicate internal portions of the microsyn and motor from making contact during launch or any other time.
2. Although preload springs were included in the original design for proper bearing positioning, the spring rate of the gimbal saddle (and the change in spring rate when the experiment saddle is mounted to the gimbal saddle) was not taken into account. Special fixturing was necessary to take this loading into account when setting the preload.

CONCLUDING REMARKS

The development tests conducted on components of the elevation drive assembly have provided assurance that the pointing accuracy, low friction, and launch lock actuation requirements for proper spacecraft operation will be achieved following the launch environment.

TABLE 1. ELEVATION DRIVE ASSEMBLY REQUIREMENTS

Parameter	Requirement
PIA mass properties	250 pounds, maximum inertia of 17 slug-ft ² about elev. gimbal
Experiment alignment	5 arcsec prelaunch 10 arcsec postlaunch
Angular excursion	± 5 degrees
Experiment Temp. Range	20°C \pm 5°C experiment
Bearing friction	6 in-oz, maximum
Flex cable torque	1 in-oz per degree, maximum
Motor torque	1.0 ft-lb, minimum
Launch Environment	
Sine Vibration	8 g max - sweep 20 to 2000 Hz
Random Vibration	max intensity 0.18 g ² /Hz
Acceleration	10 g along launch axis 3 g lateral to launch axis



Figure 1.- OSO spacecraft configuration.

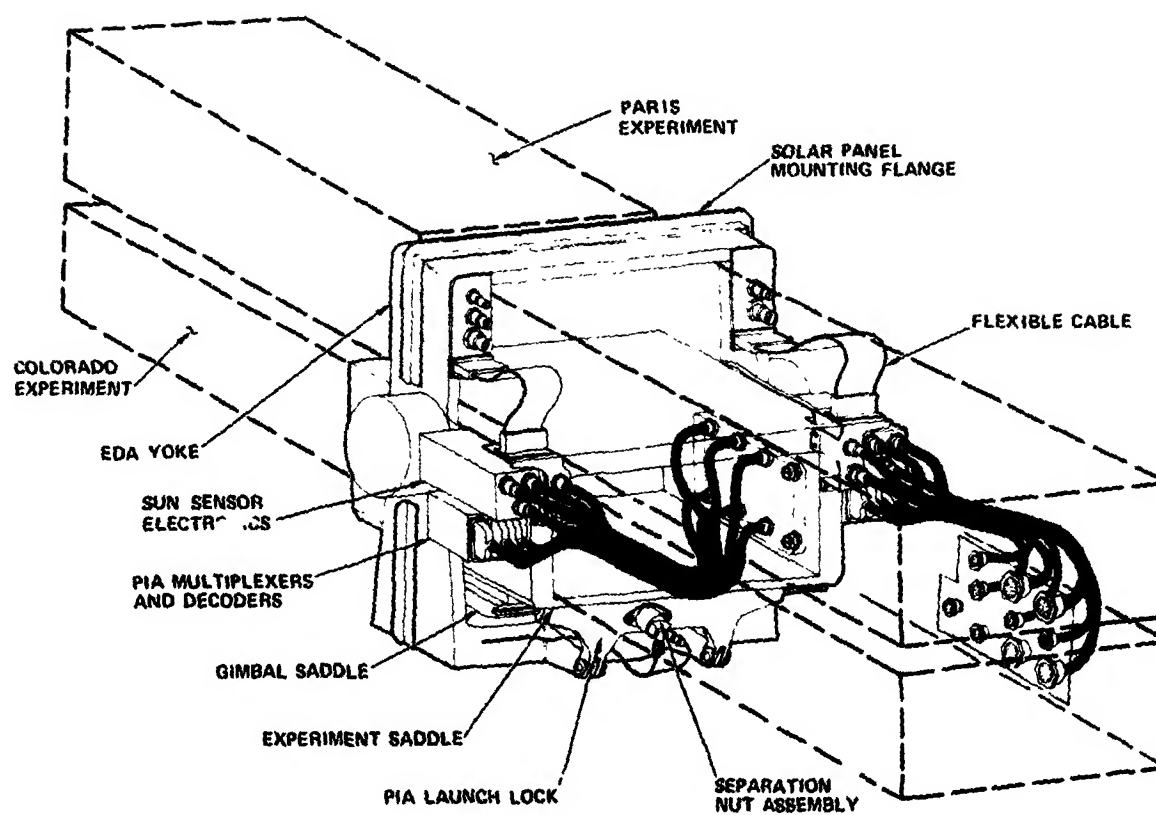


Figure 2.- EDA-PIA general arrangement.

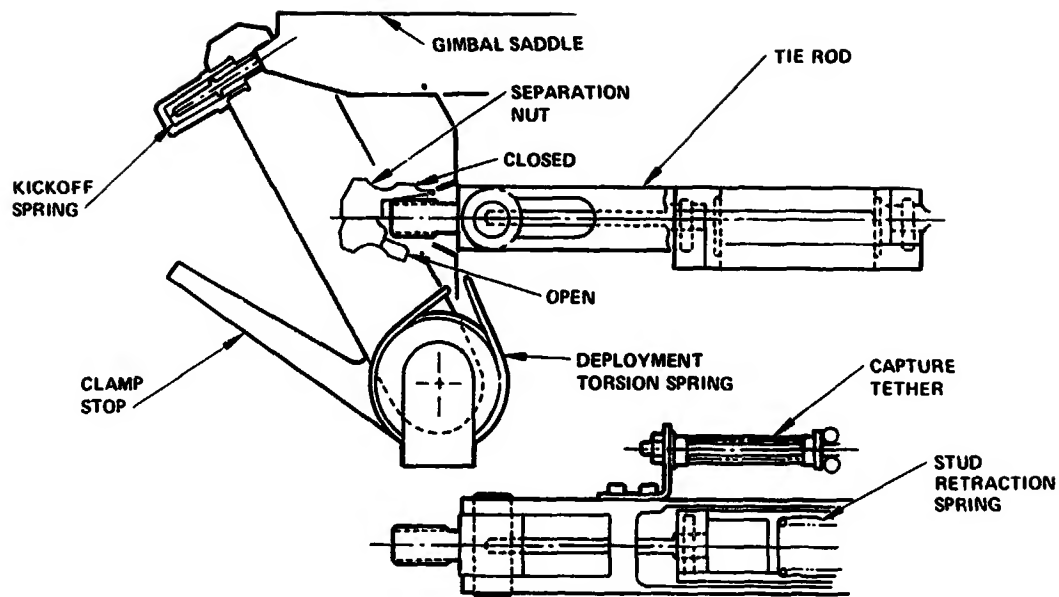


Figure 3.- PIA launch lock mechanism.

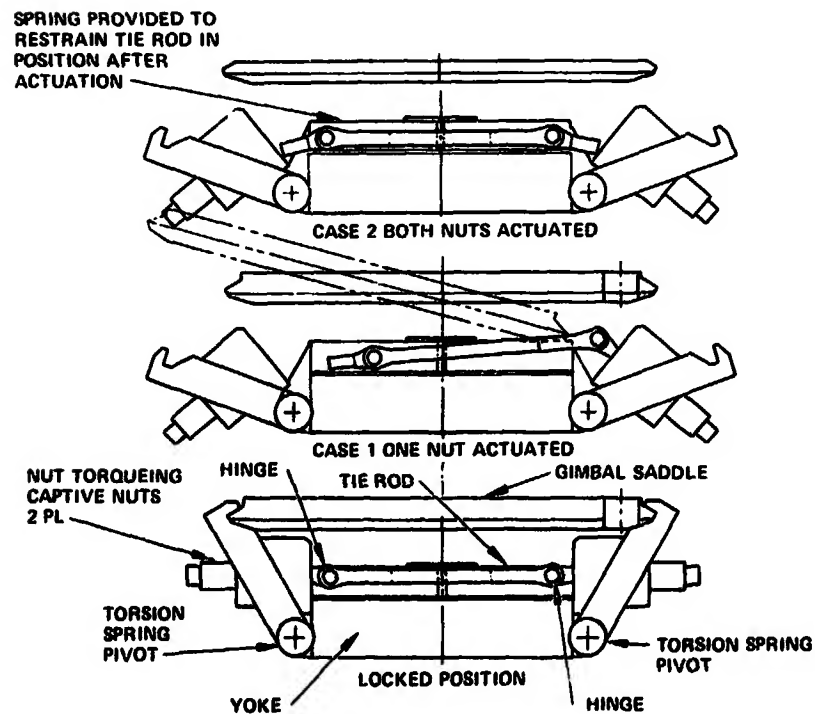


Figure 4.- PIA launch lock captive nut and tie rod.

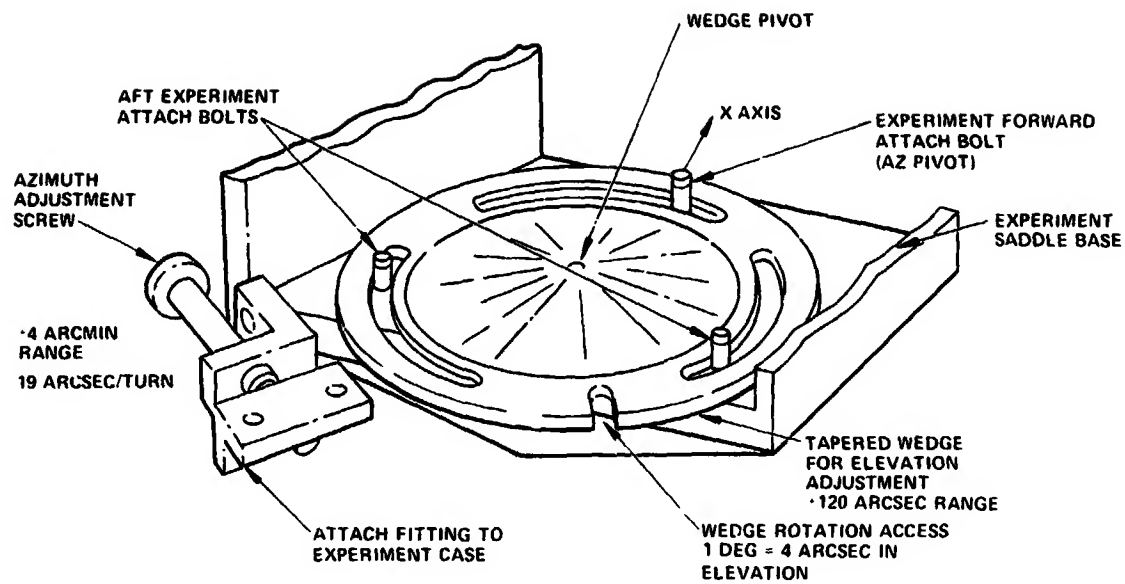


Figure 5.- Coalignment mechanism.

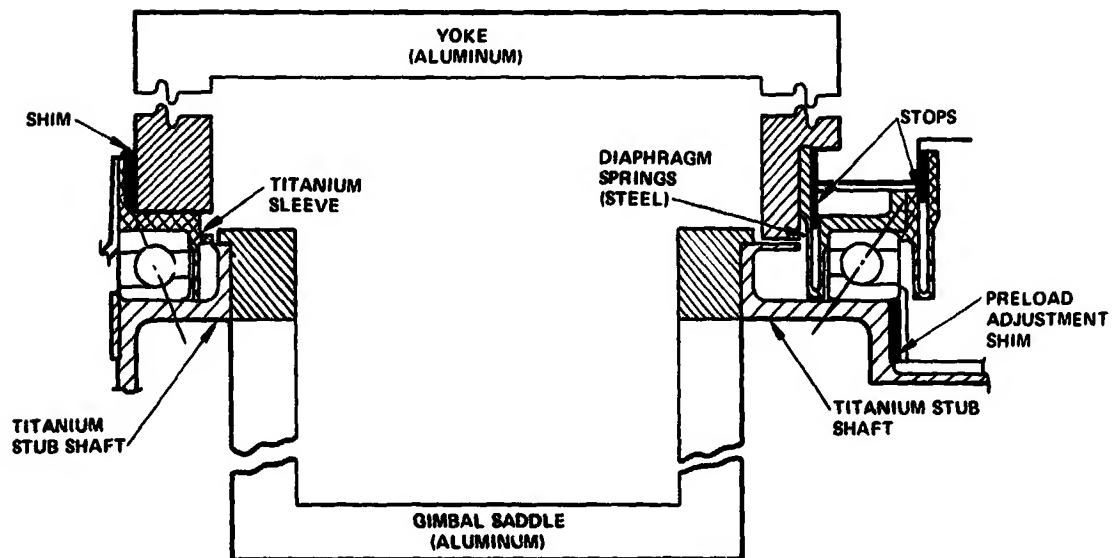


Figure 6.- EDA bearing installation.

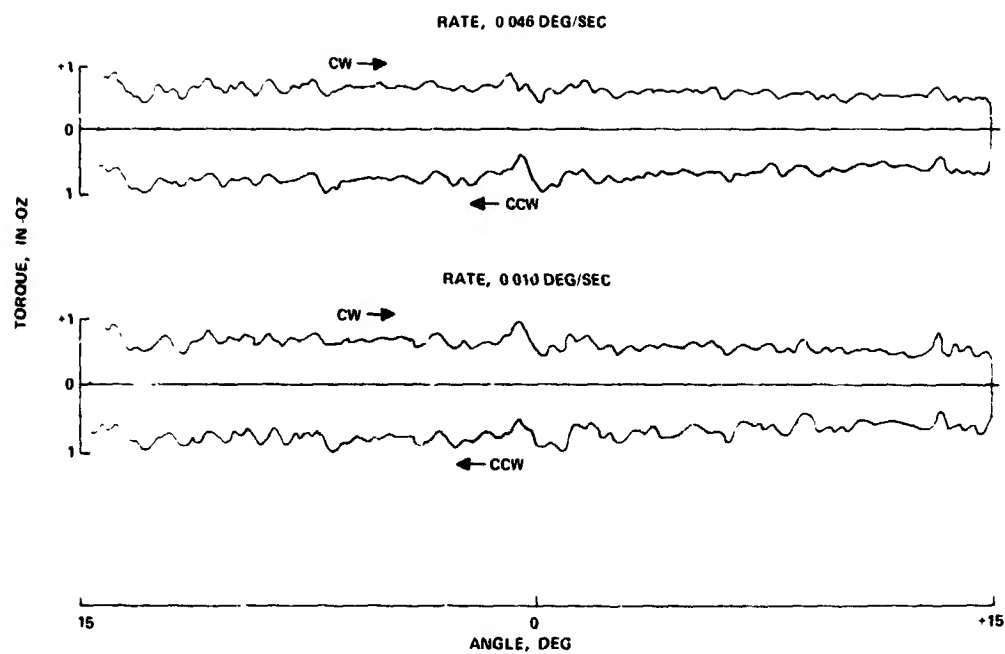


Figure 7.- Running friction test.

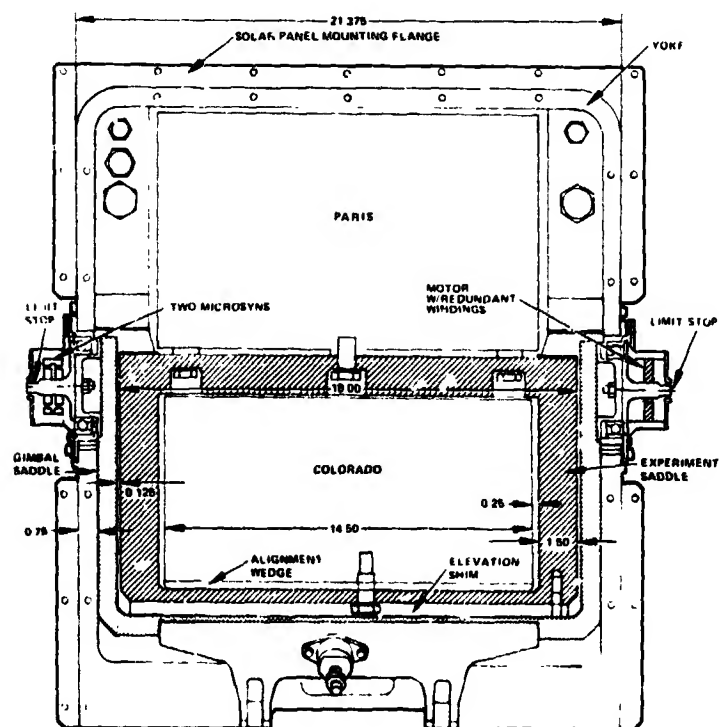


Figure 8.- Cross section of EDA with pointed experiments.
Linear dimensions are in inches.